

Methods used in AuTuMN modelling of the COVID-19 epidemic in Sri Lanka

Contents

1	Base model construction	3
1.1	Platform for infectious disease dynamics simulation	3
1.2	Base COVID-19 model	3
1.3	Age stratification	4
1.4	Clinical stratification	5
1.5	Hospitalisation	5
1.6	Infectiousness	5
1.7	Application of COVID-19-related death	6
1.8	Modelling Variants of Concern (VoC)	8
1.9	Modelling vaccine effects	8
2	Case detection and isolation	9
2.1	Determining the proportion of cases detected	9
2.2	Isolation of detected cases	10
3	Contact tracing and quarantine	10
3.1	Model adaptation	10
3.2	Contact tracing process	10
4	Implementation of non-pharmaceutical interventions	11
4.1	Isolation and quarantine	11
4.2	Community quarantine or “lockdown” measures	12
4.3	School closures/re-openings	13
4.4	Workplace closures	13
4.5	Community-wide movement restriction	13
4.6	Household contacts	13
4.7	Microdistancing	14
5	Parameters	15
5.1	Non-age-structured parameters	15
5.2	Age-specific parameters	15

6	Model Calibration	17
6.1	General approach	17
6.2	Likelihood function	17
6.3	Calibration parameters	17
7	Ordinary differential equations	19
8	Calculation of outputs	22
8.1	Incidence	22
8.2	Hospital occupancy	22
8.3	ICU occupancy	22
8.4	Seropositive proportion	22
8.5	COVID-19-related mortality	22
8.6	Notifications	22

1 Base model construction

1.1 Platform for infectious disease dynamics simulation

We developed a deterministic compartmental model of COVID-19 transmission using the AuTuMN platform, publicly available at <https://github.com/monash-emu/AuTuMN/>. Our repository allows for the rapid and robust creation and stratification of models of infectious disease epidemiology and includes pluggable modules to simulate heterogeneous population mixing, demographic processes, multiple circulating pathogen strains, repeated stratification and other dynamics relevant to infectious disease transmission. The platform was created to simulate TB dynamics, being an infectious disease whose epidemiology differs markedly by setting, such that considerable flexibility is desirable [1]. We have progressively developed the structures of our platform over recent years, and further adapted it to be sufficiently flexible to permit simulation of other infectious diseases, such as COVID-19. An similar model has been applied to several countries of the Asia-Pacific, with the application to the Philippines (without structure to represent geospatial stratification or contact tracing) previously described.[2]

1.2 Base COVID-19 model

Using the base framework of an SEIR model (susceptible, exposed, infectious, removed), we split the exposed and infectious compartments into two sequential compartments each (SEEIIR). The two sequential exposed compartments represent the non-infectious and infectious phases of the incubation period, with the latter representing the “presymptomatic” phase such that infectiousness occurs during three of the six sequential phases. For this reason, “active” is a more accurate term for the two sequential “I” compartments and is preferred henceforward. The two infectious compartments represent early and late phases of active disease, during which symptoms occur if the disease episode is symptomatic, and allow explicit representation of notification, case isolation, hospitalisation and admission to ICU. The “active” compartment also includes some persons who remain asymptomatic throughout their disease episode, such that these compartments do not map directly to either persons who are infectious or those who are symptomatic (Figure 1).

The latently infected and infectious presymptomatic periods together comprise the incubation period, with the incubation period and the proportion of this period for which patients are infectious defined by input parameters described below. In general, two sequential compartments can be used to form a gamma-distributed profile of transition to infectiousness following exposure if the

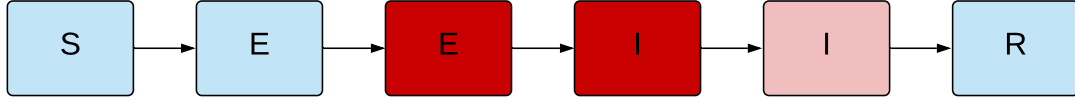


Figure 1: **Unstratified compartmental model structure.** S = susceptible, E = exposed, I = active, R = recovered/removed. Depth of pink/red shading indicates the infectiousness of the compartment.

progression rates for these two compartments are equal, although in implementing this model the relative sojourn times in the two sequential compartments usually differed. Nevertheless, the profiles implemented are broadly consistent with the empirically observed log-normal distribution of individual incubation periods [3].

The transition from early active to late active represents the point at which patients are detected (for those persons for whom detection does eventually occur) and isolation then occurs from this point forward (i.e. applies during the late disease phase only. This transition point is also intended to represent the point of admission to hospital or transition from hospital ward to intensive care for patients for whom this occurs (see Section 1.4).

1.3 Age stratification

All compartments of this base compartmental structure were stratified by age into five-year bands from 0-4 years of age through to 70-74 years of age, with the final age group being those aged 75 years and older. Heterogeneous baseline contact patterns by age were incorporated using age-specific contact rates estimated by Prem et al. 2017 [4], who combined survey response data with information on national demographic characteristics to produce age-structured mixing matrices with these age groupings. These are then modified by non-pharmaceutical interventions. Our modelled age groups were chosen to match these mixing matrices. The automatic demographic features of AuTuMN that can be used to simulate births, ageing and deaths were not implemented, because the issues considered pertain to the short- to medium-term and the immediate implementation of control strategies, for which population demographics are less relevant.

1.4 Clinical stratification

The age-stratified late exposed/incubation and both the early and late active disease compartments were further stratified into five “clinical” categories: 1) asymptomatic, 2) symptomatic ambulatory, never detected, 3) symptomatic ambulatory, ever detected, 4) ever hospitalised, never critical and 5) ever critically unwell (Figure 2). The proportion of new infectious persons entering stratum 1 (asymptomatic) is age-dependent. The proportion of symptomatic patients (strata 2 to 5) ever detected (strata 3 to 5) is set through a parameter that represents the time-varying proportion of all symptomatic patients who are ever detected (the case detection rate). Of those ever symptomatic (strata 2 to 5), a time-constant but age-specific proportion is considered to be hospitalised (entering strata 4 or 5). Of those hospitalised (entering strata 4 or 5), a fixed proportion was considered to be critically unwell (entering stratum 5, Figure 3).

1.5 Hospitalisation

For COVID-19 patients who are admitted to hospital, the sojourn time in the early and late active compartments is modified, superseding the default values of the sojourn times for these compartments. The point of admission to hospital is considered to be the transition from early to late active disease, such that the sojourn time in the late disease represents the period of time admitted to hospital. For patients admitted to ICU, admission to ICU occurs at this same transition point. For this group, the period of time hospitalised prior to ICU admission is estimated as a proportion of the early active period, such that the early active period represents both the period ambulatory in the community and the period in hospital prior to ICU admission.

1.6 Infectiousness

Asymptomatic persons are assumed to be less infectious per unit time active than symptomatic persons not undergoing case isolation (typically by around 50%, although this is varied in calibration/uncertainty analysis). Infectiousness is also decreased for persons who have been detected to reflect case isolation, and for those admitted to hospital or ICU to reflect infection control procedures (by 80% for both groups). Presymptomatic individuals are presumed to have equivalent infectiousness to those with early active COVID-19.

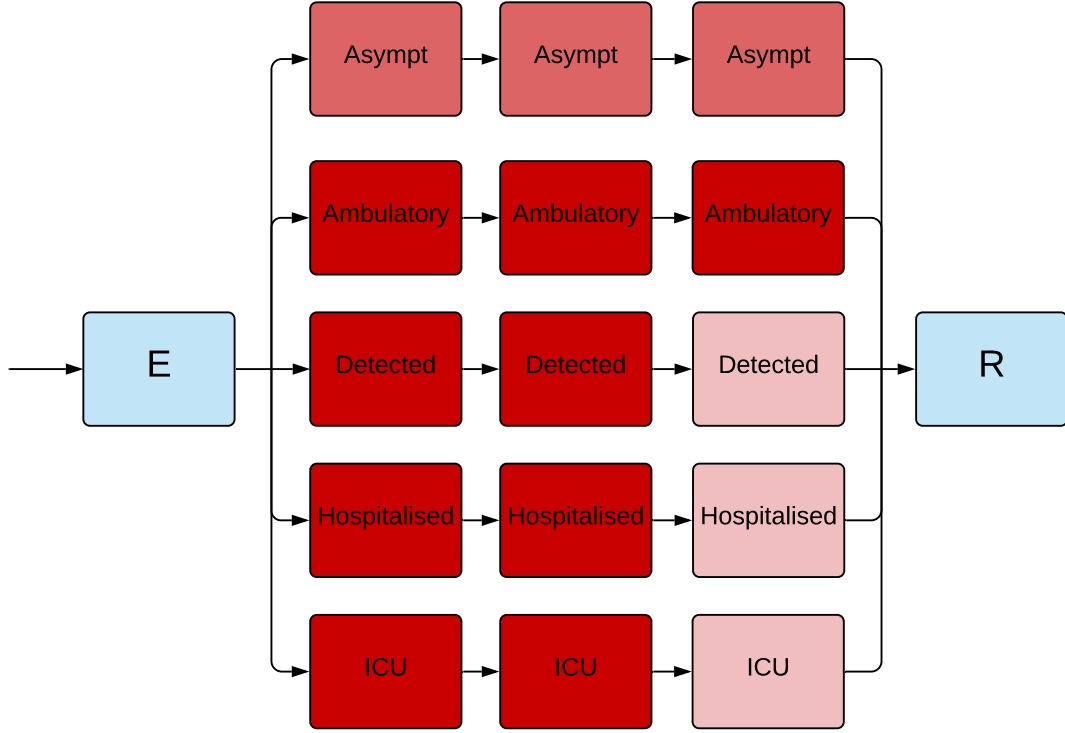


Figure 2: **Illustration of the implementation of the clinical stratification.** Depth of pink/red shading indicates the infectiousness of the compartment. Typical parameter values represented, although the infectiousness of asymptomatic persons is varied in calibration.

1.7 Application of COVID-19-related death

Age-specific infection fatality rates (IFRs) were applied and distributed across strata 4 and 5, with no deaths typically applied to the first three strata. A ceiling of 50% is set on the proportion of those admitted to ICU (entering stratum 5) who die. If the infection fatality rate is greater than this ceiling, the proportion of critically unwell persons dying was set to 50%, with the remainder of the infection fatality rate then applied to the hospitalised proportion. Otherwise, if the infection fatality rate is less than half of the absolute proportion of persons critically unwell, the infection fatality rate is applied entirely through stratum 5 (such that the proportion of critically unwell persons dying in that age group becomes <50% and the proportion of stratum 4 dying is set to zero). In the event that the infection fatality rate for an age group is greater than the total

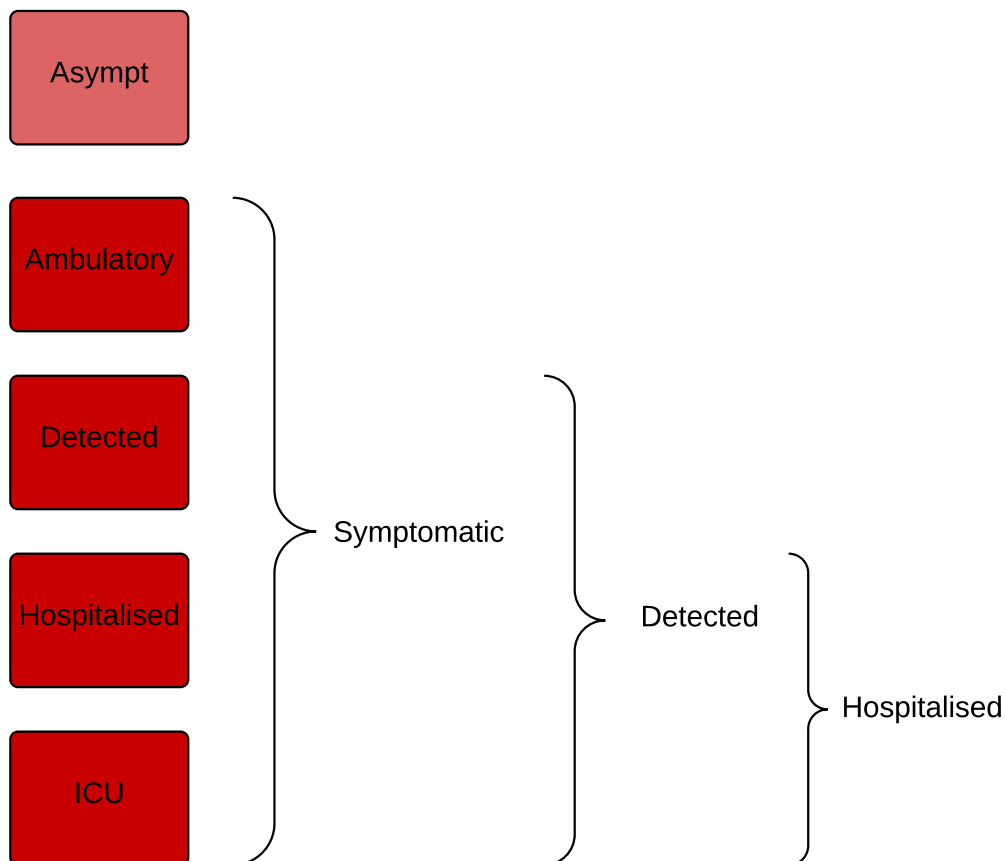


Figure 3: **Illustration of the rationale for the clinical stratification.**

proportion hospitalised (which is unusual, but could occur for the oldest age group under certain parameter configurations), the remaining deaths are assigned to the asymptomatic stratum. This approach was adopted for computational ease and is valid because the duration active for persons entering this stratum is the same as for the other non-hospitalised strata, such that the dynamics are identical to assigning the deaths to any of the first three strata. We used the age-specific IFRs previously estimated from age-specific death data from 45 countries and results from national-level seroprevalence surveys [5]. Uncertainty in the IFR estimates used in the model is incorporated as described in Section 6.

Clinical stratum	Stratum name	Pre-symptomatic	Early	Late
1	Asymptomatic	0.5	0.5	0.5
2	Symptomatic ambulatory never detected	1	1	1
3	Symptomatic ambulatory ever detected	1	1	0.2
4	Hospitalised never critical	1	1	0.2
5	Ever critically unwell	1	1	0.2

Table 1: **Illustration of the relative infectiousness of disease compartments by clinical stratification and stage of infection.** Typical parameter values displayed.

1.8 Modelling Variants of Concern (VoC)

To consider the effects of VoC on infection dynamics and the vaccination programs, we explicitly simulated three competing strains to represent the wild-type or ancestral virus, Alpha and Delta VoC strains, which are the two main VoC strains that circulated in Sri Lanka during the study period. The two VoC strains were associated with increased transmissibility relative to wild-type and the respective transmissibility levels of each VoC strain were calibrated from the model. Susceptible individuals can be infected with either the wild-type or VoC strain and infectious individuals contribute to the force of infection with their respective infecting strain only. VoC strains are seeded into the model such that 25 additional persons per day are infected with a particular VoC strain for a duration of ten days, with the time that this ten-day period commences varied during model calibration.

1.9 Modelling vaccine effects

We stratified all model compartments as either vaccinated or unvaccinated and commenced simulations with an fully unvaccinated population. With vaccination roll-out, individuals in the susceptible and recovered compartments move from “unvaccinated” to “vaccinated” at a constant rate representing vaccine administration over time. The daily rate of vaccination is calculated from the vaccine coverage achieved over a given period of time is calculated as $rate_{vac} = \frac{-\log(1-coverage)}{T}$, where coverage represents the targeted proportion of people vaccinated by the end of the roll-out period and T represents the roll-out period.

Vaccination is assumed to have two mechanisms of effect: 1) prevention of infection and 2) protection against progressing to severe infection among those infected. A particular vaccine

roll-out programme can be simulated to act through these two mechanisms simultaneously. The proportion of the effect that is attributed to preventing infection, $V_p = V_i V_e$, where $V_i \in [0, 1]$ is the infection prevention efficacy and $V_e \in [0, 1]$ is the overall efficacy (that would be observed in clinical trials). If severity prevention efficacy is denoted V_s , since $V_e = V_i + V_s(1 - V_i)$ it follows that $V_s = \frac{V_e(1-V_p)}{1-V_pV_e}$. For the component of the vaccine effect attributed to infection prevention, the infection risk of vaccinated individuals is reduced by $(1 - V_i)$. Severity-preventing vaccination reduces the infection fatality rate (IFR) and the probability that an infected individual experiences symptomatic disease. Thus, the vaccine efficacy parameter pertaining to disease severity prevention modifies the splitting proportions of infected individuals between the different clinical categories and the rate of COVID-19-related mortality.

2 Case detection and isolation

2.1 Determining the proportion of cases detected

We calculate a time-varying case detection rate, being the proportion of all symptomatic cases (clinical strata 2 to 5) that are detected (clinical strata 3 to 5). This proportion is informed by the number of tests performed using the following formula:

$$CDR(time) = 1 - e^{-shape \times tests(time)}$$

$time$ is the time in days from the 31st December 2019 and $tests(time)$ is the number of tests per capita done on that date. To determine the value of the shape parameter, we solve this equation based on the assumption that a certain daily testing rate $tests(t)$ is associated with a certain $CDR(t)$. Solving for $shape$ yields:

$$shape = \frac{-\log(1 - CDR(t))}{tests(t)}$$

That is, if it is assumed that a certain daily per capita testing rate is associated with a certain proportion of symptomatic cases detected, we can determine $shape$. As this relationship is not well understood and unlikely to be consistent across all settings, we vary the CDR that is associated with a certain per capita testing rate during uncertainty/calibration. Given that the CDR value can be varied widely, the purpose of this is to incorporate changes in the case detection rate that reflect the empirical historical profile of changes in testing capacity over time.

The proportion of persons entering clinical stratum 3 is calculated once the CDR is known, along with the proportion of all incident cases hospitalised (strata 4 and 5).

2.2 Isolation of detected cases

As described in the Section 1.4 above, as infected persons progress from the early to the late stage of active COVID-19, infectious is reduced for those in the detected strata (3 to 5) to reflect case isolation.

3 Contact tracing and quarantine

3.1 Model adaptation

We simulate quarantining of persons identified as first degree contacts of COVID-19 patients explicitly through stratification of the compartments representing active COVID-19. That is, the compartments representing both phases of the incubation period and both phases of active COVID-19 are duplicated and stratified, with model strata referred to as “traced” and “untraced”. In model initialisation, all infectious seed is assigned to the untraced stratum. All newly infected persons commence their incubation period in the untraced stratum of the early incubation period. As for isolated and hospitalised patients, those undergoing quarantine have their infectiousness reduced by 80%.

3.2 Contact tracing process

Identification of infected persons through contact tracing is assumed to apply to those in their early incubation period, with flows added to the model that transition persons during their incubation period from the untraced to the traced stratum of this compartment type. The rate of transition from the untraced to the traced stratum of the early incubation period is determined by the proportion of contacts traced. It is assumed that only the contacts of identified cases can be traced, such that the case detection rate (the proportion of symptomatic cases detected) is considered the ceiling for the proportion of contacts traced. The proportion of contacts of identified cases that is traced is multiplied by the proportion of contacts whose index is detected to determine the proportion of all persons entering the incubation period who are traced. The proportion of contacts with detected index, $u(t)$, is calculated as the relative contribution of ever-detected infectious individuals to the total force of infection, given as:

$$u(t) = \frac{\sum_{c \in \mathcal{C}} \sum_{s \in \mathcal{D}} prev_{c,s}(t) \times inf_{c,s}}{\sum_{c \in \mathcal{C}} \sum_{s \in \mathcal{S}} prev_{c,s}(t) \times inf_{c,s}},$$

where \mathcal{C} is the set of infectious compartments, \mathcal{S} represents all clinical strata and $\mathcal{D} \subset \mathcal{S}$ is the

list of detected clinical strata. The prevalence of infectious compartment c in clinical stratum s at time t is represented by $prev_{c,s}(t)$, and $inf_{c,s}$ is the relative infectiousness of compartment c in clinical stratum s .

The proportion of contacts of identified cases that is traced, $q(t)$, is considered to decrease as the severity of the COVID-19 epidemic increases, because we expect contact tracing to decline in efficiency as more cases are identified. That is, we assume that contact tracing is universal as COVID-19 prevalence approaches zero and declines exponentially with increasing prevalence. The relationship between the proportion of contacts of identified patients who are quarantined and prevalence is given as:

$$q(t) = e^{-prev(t) \times \tau}$$

Rather than estimate τ directly, we estimate the more intuitive quantity of the proportion of contacts of identified patients who would be quarantined at a particular prevalence. Solving for the previous equation for τ , we obtain:

$$\tau = \frac{-\log(q(t))}{prev(t)}$$

or $\tau = \frac{-\log(q_0)}{prev_0}$ at a specific prevalence that accords with a particular value of q . Fixing $prev_0$ at 10^{-3} , we can vary q_0 in calibration as the proportion of contacts of identified cases detected at a prevalence of one active case per thousand population.

Finally, $q(t) \times u(t)$ gives the proportion of all infected persons who are traced. This proportion of persons entering their early latent period transition to the equivalent compartment in the traced stratum before proceeding to the late latent period.

4 Implementation of non-pharmaceutical interventions

A major part of the rationale for the development of this model was to capture the past impact of non-pharmaceutical interventions (NPIs) and produce future scenarios projections with the implementation or release of such interventions.

4.1 Isolation and quarantine

For persons who are identified with symptomatic disease and enter clinical stratum 3, self-isolation is assumed to occur and their infectiousness is modified as described above. The proportion of ambulatory symptomatic persons effectively identified through the public health response by any means is determined by the case detection rate as described above.

4.2 Community quarantine or “lockdown” measures

For all NPIs relating to reduction of human mobility or “lockdown” (i.e. all NPIs other than isolation and quarantine), these interventions are implemented through dynamic adjustments to the age-assortative mixing matrix. The baseline mixing matrices of Zhang et al. [6] are based on contact patterns of 965 individuals during the period of 2017/18 in Shanghai City, China. The matrices also have the major advantage of allowing for disaggregation of total contact rates by location, i.e. home, work, school and other locations. This disaggregation allows for the simulation of various NPIs in the local context by dynamically varying the contribution of each location to reflect the historical implementation of the interventions.

For each location L (home, school, work, other locations) the age-specific contact matrix $\mathbf{C}^L = (c_{i,j}^L) \in \mathbb{R}_+^{16 \times 16}$ is defined such that $c_{i,j}^L$ is the average number of contacts that a typical individual aged i has with individuals aged j . The original matrices from China are denoted $\mathbf{Q}^L = (q_{i,j}^L) \in \mathbb{R}_+^{16 \times 16}$, where $q_{i,j}^L$ is defined using the same convention as for $c_{i,j}^L$. The matrices \mathbf{Q}^L were extracted using the R package “socialmixr” (v 0.1.8) and to obtain the contact matrices relating to Sri Lanka (\mathbf{C}^L), these were then adjusted to account for age distribution differences between Sri Lanka and China.

Let π_j denote the proportion of people aged j in Malaysia, and ρ_j the proportion of people aged j in China. The contact matrices \mathbf{C}^L were obtained from:

$$c_{i,j}^L = q_{i,j}^L \times \frac{\pi_j}{\rho_j}.$$

The overall contact matrix results from the summation of the four location-specific contact matrices: $C_0 = C_H + C_S + C_W + C_L$, where C_H , C_S , C_W and C_L are the age-specific contact matrices associated with households, schools, workplaces and other locations, respectively.

In our model, the contributions of the matrices C_S , C_W and C_L vary with time such that the input contact matrix can be written:

$$C(t) = C_H + s(t)^2 C_S + w(t)^2 C_W + l(t)^2 C_L$$

The modifying functions are each squared to capture the effect of the mobility changes on both the infector and the infectee in any given interaction that could potentially result in transmission. The modifying functions incorporate both macro-distancing and microdistancing effects, depending on the location.

4.3 School closures/re-openings

Reduced attendance at schools is represented through the function $s(t)$, which represents the proportion of all school students currently attending on-site teaching. If schools are fully closed, $s(t) = 0$ and C_S does not contribute to the overall mixing matrix $C(t)$. $s(t)$ is calculated through a series of estimates of the proportion of students attending schools, to which a smoothed step function is fitted. Note that the dramatic changes in this contribution to the mixing matrix with school closures/re-openings is a more marked change than is seen with the simulation of policy changes in workplaces and other locations (which are determined by empiric data and so do not vary so abruptly or reach a value of zero).

4.4 Workplace closures

Workplace closures are represented by quadratically reducing the contribution of workplace contacts to the total mixing matrix over time. This is achieved through the scaling term $w(t)^2$ which modifies the contribution of C_W to the overall mixing matrix $C(t)$. The profile of the function $w(t)$ is set by fitting a polynomial spline function to Google mobility data for workplace attendance (Table 2).

4.5 Community-wide movement restriction

Community-wide movement restriction (or “lockdown”) measures are represented by proportionally reducing the contribution of the other locations contacts to the total mixing matrix over time. This is achieved through the scaling term $l(t)^2$ which modifies the contribution of C_L to the overall mixing matrix $C(t)$. The profile of the function $l(t)$ is set by fitting a polynomial spline function to an average of Google mobility data for various locations, as indicated in Table 2.

4.6 Household contacts

The contribution of household contacts to the overall mixing matrix $C(t)$ is fixed over time. Although Google provides mobility estimates for residential contacts, the nature of these data are different from those for each of the other Google mobility types. They represent the time spent in that location, opposed to other categories, which measure a change in total visitors rather than the duration. The daily frequency with which people attend their residence is likely to be close to one and we considered that household members likely have a daily opportunity for infection with each

other household member. Therefore, we did not implement a function to scale the contribution of household contacts to the mixing matrix with time.

location	Approach	Google mobility types
School	Policy response	Not applicable
Household	Constant	Not applicable
Workplace	Google mobility	Workplace
Other locations	Google mobility	Unweighted average of: <ul style="list-style-type: none"> • Retail and recreation • Grocery and pharmacy • Parks • Transit stations

Table 2: Mapping of Google mobility data to contact locations.

4.7 Microdistancing

Interventions other than those that prevent people coming into contact with one another are thought to be important to COVID-19 transmission and epidemiology, such as maintaining interpersonal physical distance and the wearing of face coverings. We therefore implemented a “microdistancing” function to represent reductions in the rate of effective contact that is not attributable to persons visiting specific locations and so is not captured through Google mobility data. This microdistancing function reduces the values of all elements of the mixing matrices by a certain proportion and is applied to all non-household locations. These time-varying functions multiplicatively scale the location-specific contact rate modifiers $s(t)$, $w(t)$ and $l(t)$. The microdistancing function for non-household locations is given as:

$$micro(t) = \frac{upper_{asympt}}{2} (\tanh(0.05(t - inflection_{time})) + 1)$$

where, $upper_{asympt}$ represents the final value of the microdistancing component and $inflection_{time}$ is the time when inflection occurs in the scaling curve.

5 Parameters

5.1 Non-age-structured parameters

This section currently remains under development.

5.2 Age-specific parameters

Age-structured parameters are presented in Table 3.

Age group (years)	Clinical fraction ^a	Relative suscepti- bility to infection	Infection fatality rate	Proportion of symptomatic patients hospi- talised
0 to 4	0.533	0.36	3×10^{-5}	0.0777
5 to 9	0.533	0.36	1×10^{-5}	0.0069
10 to 14	0.533	0.36	1×10^{-5}	0.0034
15 to 19	0.533	1	3×10^{-5}	0.0051
20 to 24	0.679	1	6×10^{-5}	0.0068
25 to 29	0.679	1	1.3×10^{-4}	0.0080
30 to 34	0.679	1	2.4×10^{-4}	0.0124
35 to 39	0.679	1	4.0×10^{-4}	0.0129
40 to 44	0.679	1	7.5×10^{-4}	0.0190
45 to 49	0.679	1	1.21×10^{-3}	0.0331
50 to 54	0.679	1	2.07×10^{-3}	0.0383
55 to 59	0.679	1	3.23×10^{-3}	0.0579
60 to 64	0.803	1	4.56×10^{-3}	0.0617
65 to 69	0.803	1.41	1.075×10^{-2}	0.1030
70 to 74	0.803	1.41	1.674×10^{-2}	0.1072
75 and above	0.803	1.41	5.748×10^{-2} , ^b	0.0703
Source/ rationale	Table 1 of systematic review and meta-analysis with appropriate accounting for testing during the pre-symptomatic period [7].	Conversion of odds ratios presented in Table S15 of Zhang et al. 2020 to relative risks using data presented in Table S14 of the same study [8]. ^c	Estimated from pooled analysis of data from 45 countries from Table S3 of O'Driscoll et al [5]. Values consistent with previous estimates using serosurveys performed in Spain [9].	Estimates from the Netherlands as the first wave of infections declined from 4th May to 21st July [10].

Table 3: **Age-stratified parameters not varied during calibration, or varied through a common multiplier.** ^aProportion of incident cases developing symptoms. ^bWeighted average of IFR estimates for 70 to 79 and 80 and above age groups. ^cNote the relative magnitude of these values are similar to those estimated by the analysis we use to estimate the age-specific clinical fraction.

6 Model Calibration

We calibrated the Sri Lanka national model to two targets: case notifications and infection-related deaths. Further details on the calibration procedure are described below and the prior distributions of epidemiological calibration parameters are described in (Table 4).

6.1 General approach

The model was calibrated using an adaptive Metropolis (AM) algorithm. In particular, we used the algorithm based on adaptive Gaussian proposal functions proposed by Haario et al. to sample parameters from their posterior distributions. We ran seven independent AM chains and combined the samples of the seven chains to project epidemic trajectories over time. The definitions of the prior distributions and the likelihood are detailed as follows.

6.2 Likelihood function

Likelihood functions are derived from comparing model outputs to target data at each time point nominated for calibration. The dispersion parameters of these distribution are included as calibration parameters and varied during the calibration approach to improve calibration efficiency.

6.3 Calibration parameters

Epidemiological calibration parameters are described in (Table 4).

Parameter name	Distribution type	Distribution Parameters
Incubation period	Truncated normal	Mean 5.5 days, standard deviation 0.97 days, truncation <1 day
Infectious period (for clinical strata 1 to 3)	Truncated normal	Mean 6.5 days, standard deviation 0.77 days, truncation <4 days
Risk of infection per contact	Uniform	0.018 to 0.028
Infectious seed	Uniform	Range 150 to 400
Case detection rate at testing rate of 1 test per 10, 000 per day (proportion)	Uniform	Range 0.04 to 0.18
Increased transmissibility of VoC strains	Uniform	1.5 to 3.0
Start time of VoC emergence	Uniform	Jan 14, 2021 to Mar 15, 2021

Table 4: Epidemiological calibration parameters

7 Ordinary differential equations

For the clearest description of the model, we refer the reader to our code repository, because our object-oriented approach to software development is intended to be highly transparent and readable. For those who prefer dynamical systems such as those presented in the form of ordinary differential equations, we present the following.

$$\begin{aligned}
\frac{dS_a}{dt} &= -\lambda_a(t) \times \sigma_a \times S_a \\
\frac{dE_a}{dt} &= \lambda_a(t) \times \sigma_a \times S_a - \alpha E_a \\
\frac{dP_{a,c}}{dt} &= p_{a,c}(t) \times \alpha E_a - \nu P_{a,c} \\
\frac{dI_{a,c}}{dt} &= \nu P_{a,c} - \gamma_c I_{a,c} \\
\frac{dL_{a,c}}{dt} &= \gamma_c I_{a,c} - \delta_{a,c} L_{a,c} - \mu_{a,c} L_{a,c} \\
\frac{dR_a}{dt} &= \sum_c \delta_{a,c} L_{a,c}
\end{aligned}$$

where

$$\begin{aligned}
\lambda_a &= \beta \left[\sum_{j,c} \frac{\epsilon \times P_j}{N_j} \times C_{a,j}(t) + \sum_{j,c} \frac{I_{j,c} \times \iota_c + L_{j,c} \times \kappa_c}{N_j} \times C_{a,j}(t) \right] \\
\sum_c p_{a,c}(t) &= 1, \forall t \in \mathbb{R} \\
\mathbf{C}_0 &= \mathbf{C}_H + \mathbf{C}_S + \mathbf{C}_W + \mathbf{C}_L \\
\mathbf{C}(t) &= h(t) \times \mathbf{C}_H + s(t) \times \mathbf{C}_S + w(t) \times \mathbf{C}_W + l(t) \times \mathbf{C}_L \\
l(t) &= \frac{re(t) + gr(t) + pa(t) + tr(t)}{4}
\end{aligned}$$

Symbol	Explanation
S	Persons susceptible to infection
E	Persons in the non-infectious incubation period
P	Persons in the incubation period
I	Persons in the early active disease period, before isolation or hospitalisation may occur
L	Persons in the late active disease period, after isolation or hospitalisation may have occurred
R	Persons in the recovered period, from which re-infection cannot occur

Symbol	Explanation
t	Time
a	Compartment of age group a
c	Compartment of clinical stratification c
σ	Relative susceptibility to infection
α	Rate of progression from non-infectious to infectious incubation period
ν	Rate of progression from infectious incubation to early active disease
γ	Rate of progression from early active disease to late active disease
μ	Rate of disease-related death
ϵ	Relative infectiousness of pre-symptomatic compartment
ι	Clinical stratification infectiousness vector for early active compartment
κ	Clinical stratification infectiousness vector for late active compartments
β	Probability of infection per contact between an infectious and susceptible individual
j	Infectious populations
p	Proportion progressing to each clinical stratification
C	Mixing matrix
H	Household contribution to mixing matrix
W	Workplace contribution to mixing matrix
O	Other locations contribution to mixing matrix
S	Schools contribution to mixing matrix
l	Other locations macrodistancing function of time
w	Function fit to Google mobility data for workplaces
s	Function fit to Google mobility data for schools
re	Function fit to Google mobility data for retail and recreation
gr	Function fit to Google mobility data for grocery and pharmacy
pa	Function fit to Google mobility data for parks
tr	Function fit to Google mobility data for transit stations

8 Calculation of outputs

8.1 Incidence

Incidence is calculated as any transitions into the early active compartment (“ I ”).

8.2 Hospital occupancy

Hospitalisation numbers are not reported in the case of Sri Lanka, because the approach to hospitalisation in the country differ considerably from that adopted in the other countries to which the AuTuMN model is applied. Therefore, our approach to simulating hospitalisations is not applicable to Sri Lanka.

8.3 ICU occupancy

This is calculated as all persons in the late active compartment in clinical stratum 5.

8.4 Seropositive proportion

This is calculated as the proportion of the population in the recovered (“ R ”) compartment. Although very similar numerically to the attack rate, persons who died of COVID-19 are not included in the denominator.

8.5 COVID-19-related mortality

This is calculated as all transitions representing death, exiting the model. This is implemented as depletion of the late active compartment.

8.6 Notifications

Local case notifications are calculated as transitions from the early to the late active compartment for clinical strata 3 to 5.

References

- [1] J. M. Trauer et al. Modular programming for tuberculosis control, the "autumn" platform. *BMC Infect Dis*, 17(1):546, 2017.
- [2] J. M. Caldwell et al. Understanding covid-19 dynamics and the effects of interventions in the philippines: A mathematical modelling study. *The Lancet Regional Health – Western Pacific*, 14, 2021.
- [3] C. McAloon et al. Incubation period of covid-19: a rapid systematic review and meta-analysis of observational research. *BMJ Open*, 10(8):e039652, 2020.
- [4] K. Prem et al. Projecting social contact matrices in 152 countries using contact surveys and demographic data. *PLoS Comput Biol*, 13(9):e1005697, 2017.
- [5] M. O’Driscoll et al. Age-specific mortality and immunity patterns of sars-cov-2. *Nature*, 590(7844):140–145, 2021.
- [6] J. Zhang et al. Patterns of human social contact and contact with animals in shanghai, china. *Scientific Reports*, 9(1):15141, 2019.
- [7] P. Sah et al. Asymptomatic sars-cov-2 infection: A systematic review and meta-analysis. *Proceedings of the National Academy of Sciences*, 118(34):e2109229118, 2021.
- [8] J. Zhang et al. Changes in contact patterns shape the dynamics of the covid-19 outbreak in china. *Science*, 368(6498):1481–1486, 2020.
- [9] M. Pollán et al. Sars-cov-2 seroprevalence in spain - authors’ reply. *Lancet*, 396(10261):1484–1485, 2020.
- [10] Wekelijkse update epidemiologische situatie COVID-19 in Nederland — RIVM.